International Journal of Recent Technology and Engineering (IJRTE)
ISSN: 2277-3878 (Online), Volume-5 Issue-3, July 2016

Role of Ball and Coating Materials under Un-lubricated Condition

Suresha Gowda M. V., Ranganatha S., Vidyasagar H. N.

Abstract: ***The performance, reliability and load transferring capabilities of bearing elements are very important in industrial applications. The newer design of high speed machines demands better bearing system. The reliability is of primary importance in case of bearing elements used in aerospace industries. Exhaustive studies have been carried out by different researchers under two extreme conditions. One is using a fluid as lubricants which do not bear shear loads. The other extreme were using hard coatings which bears enormous amount of shear loads. In the present investigation an attempt has been made to understand the kinematics of deformation of balls and coatings which are not as hard as conventional coatings without lubricants. Different ball materials like case hardened carbon steel, high carbon high chromium steel and stainless steel, case hardened carbon steel and high carbon high chromium steel balls were coated with tin and case hardened carbon steel and stainless steel balls were coated with zinc by electroplating coating technique. The thickness of the coating was maintained at 25 µm. Four ball test rig was used to simulate the field condition. The experiments were conducted without lubricants. The normal loads were 100N, 300N and 500N respectively for case hardened carbon steel and high carbon high chromium steel, run for a period of 5 minutes. The normal loads were 50N, 75N and 100N respectively for stainless steel and run for a period of 5 minutes. The frictional load and normal load were monitored and co-efficient of friction was estimated. The wear scar was studied under scanning electron microscope. The co-efficient of friction was found to be dependent on normal load and type of coating material. The co-efficient of friction was found to be minimum of value 0.27 for a maximum normal load of 500N for tin coatings and 0.41 for a maximum load of 500N for zinc coatings. The morphology of wear scar studied in scanning electron microscope explains the dependency of co-efficient of friction on normal load and different coating materials.***

Keywords: Rolling contact fatigue, four ball tester, Coatings.

I. INTRODUCTION

The life of machine element which transfers load and motion are very important. In specific the performance of journal bearings is of more industrial importance since these elements are used in machineries which run at very high speed and in hostile environment. The roller bearings are intermediate between the rotor and housing of the bearing.

Revised Manuscript Received on 30 July 2016.
* Correspondence Author
Suresha Gowda M .V Department of Mechanical Engineering, University Visweswaraya College of Engineering, Bangalore, Karnataka, India.
Dr. Ranganatha S Department of Mechanical Engineering, University Visweswaraya College of Engineering, Bangalore, Karnataka, India.
Dr. Vidyasagar H . N Department of Mechanical Engineering, University Visweswaraya College of Engineering, Bangalore, Karnataka, India.

They accommodate the velocity and displacement between the static bearing and high velocity rotor. The performance of the roller is important from the point of reliability, accommodating shear loads, transferring the compressive loads and economy of the product.

Attempts have been made to improve the life of these elements using different kinds of lubricants. Studies have been carried out using different lubricating materials and different lubricating domains. The domain studied are fully developed, mixed and boundary regimes [1]. The results showed that lubrication regime had a significant effect on performance of bearings. The lubricants depending on the regime were found to lead to different types of failure [2].

Attempts also have been made to provide hard coatings to improve the performance and reliability of the bearing element. The different coatings techniques employed were thermal spraying (TS), physical vapor deposition (PVD) and chemical vapor deposition (CVD). Faraday [3] develops the PVD process. Titanium coatings were deposited using the PVD process for improving the wear resistance. The deposition process resulted in discontinuities such as pore, thermal stress induced cracks and oxylamide oxide lamellas are in completely molten particles. These defects were reported to be depending on process parameters involved in spraying [4-7].

Different authors tried to understand the performance of thermally coated bearing elements [8-11]. They found that improved microstructure and fracture toughness resulted in better performance of the rolling elements.

Attempts are also having been made to study the effect of different coating materials [12]. Thermally sprayed ceramic coating and metal coatings were tested in the laboratory. The results indicated metal coatings perform well compared to ceramic coatings. The failure mechanisms review formations of blisters which lead to coating delamination. Mixed carbide coatings were also tried. The mixed carbides resulted in better performance. Aluminum oxide coatings were also tried but they were found to be inferior compared to carbide titanium based coatings. Role of coating thickness were also studied [13-16]. The thickness of the coating was found to change the delamination from interfacial to cohesive. The coatings were imparted at high temperature, which led to thermal stresses [17-19]. The stresses were found to be tensile in some methods and compressive in other methods.

Studies have been carried out to understand the failure mechanisms. The mechanisms were found to be dependent on defects within the coatings, microstructure of the coatings and density of the coatings [20-26].

Published By:
Blue Eyes Intelligence Engineering and Sciences Publication (BEIESP)

Suresh Gowda et al conducted experiments in four ball test rig for identifying the role of materials on deformation, damages and role of coating on case hardened carbon steel ball and they found that the hardness of the material and normal loads control the deformation and damages of load bearing elements [27-28].

The literatures reveal that attempts to accommodate the discontinuity in displacement and velocity are addressed by two approaches. One being the liquid lubricant which resists no shear stresses and transfer the compressive loads. The second approach is to give a coating which will have sufficiently larger shear strength which prevents the loss of material. In the present investigation an attempt has been made to understand the role of ball and coatings which are not as stronger as conventional coatings but to some extent resist the shear stress unlike liquid lubricants which do not resists shear loads.

II. EXPERIMENTAL DETAILS

A. Material

Tests have been conducted for understanding the deformation characteristics of rolling elements and effect of coating on rolling elements using four ball test rig. Case hardened carbon steel, high carbon high chromium steel and stainless steel balls were used. Also case hardened carbon steel and high carbon high chromium steel balls were coated with tin and case hardened carbon steel and stainless steel balls were coated with zinc were used. The coatings have been carried out by standard electroplating technique. The thickness of the plating was maintained at 25 µm. The chemical composition, dimension and physical properties of different materials used as balls are shown in Table 1 and 2.

Table 1. Chemical composition of the test balls.

Material	%C	%Si	%Mn	%P	%S	%Cr
High carbon high chromium steel	0.95-1.1	0.35	0.2-0.5	0.025	0.05	1.3-1.6
Case hardened carbon steel	0.08-0.13	0.10-0.35	0.3-0.6	0.04	0.05	-
Stainless steel	0.08	0.75	2	0.045	0.03	18-20

Table 2. Dimension and physical properties of test balls.

Property	High carbon high chromium steel	Case hardened carbon steel	Stainless steel
Diameter (mm)	12.7	12.7	12.7
Surface roughness *Ra* (µm)	0.024	0.024	0.024
Hardness (HRC)	60	60	39
Modulus of elasticity(GPa)	200	200	200
Poisson's ratio	0.3	0.3	0.3

The yield strength of different coating materials are shown in Table 3.

Table 3. Yield strength of different coating materials.

Material	Yield strength (MPa)
Tin	9-14
Zinc	200

Experiments were conducted using four ball test rig as per ASTM (D 4172) standards. The schematic diagram of test rig is shown in **Fig.1.** The test rig was loaded with four balls, three at the bottom and one on top. All the balls are washed with acetone and dried to maintain the surfaces free from impurities. The bottom three balls were held firmly in a ball pot without lubricant under test and pressed against the top ball. The top ball was made to rotate at the desired speed while the bottom three balls were pressed against it.

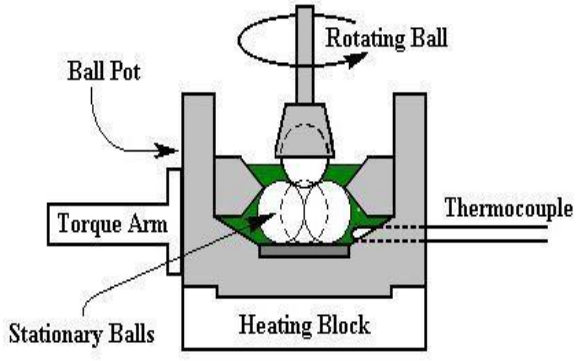

Fig.1 Schematic Diagram of Four Ball Test Rig

B. Test Procedure

A normal load of 1kg (100N) was applied and experiment was conducted by rotating the upper ball at a speed of 500 rpm. The experiment was conducted for running over 5 minutes. The ambient temperature was maintained at 75 ºC. The same procedure was repeated for loads of 3kg and 5kgs. In case of stainless steel experiments were conducted for loads of 50 N, 75 N and 100 N. Experiments in case of stainless steel could not be conducted at load greater than 100 N because of seizure of balls during the test. The normal load, frictional force and co-efficient of friction were monitored and recorded on a personal computer. The balls after test were carefully taken out of the test rig and the wear scar which is due to deformation of material of the balls were studied under scanning electron microscope.

III. RESULTS AND DISCUSSIONS

A. Effect of ball material without lubricant

The typical plots showing dependency of co-efficient of friction with time for experiments where case hardened carbon steel, high carbon high chromium steel and stainless steel balls without lubricant are shown in Fig. 2 (a) to (c)

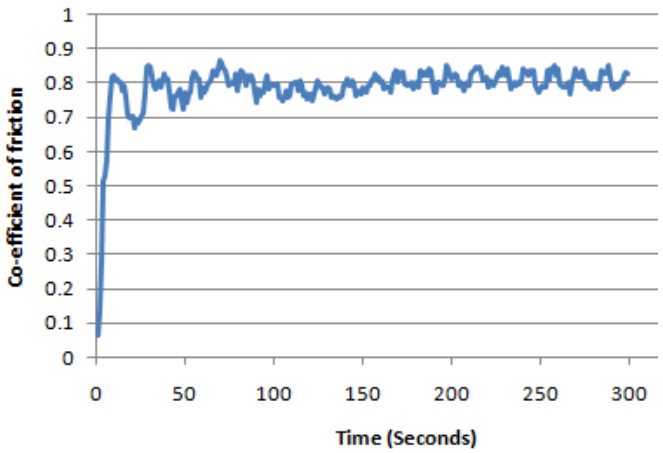

Fig. 2 (a) Dependency of co-efficient of friction with time. Material; Case hardened carbon steel Load; 100N.

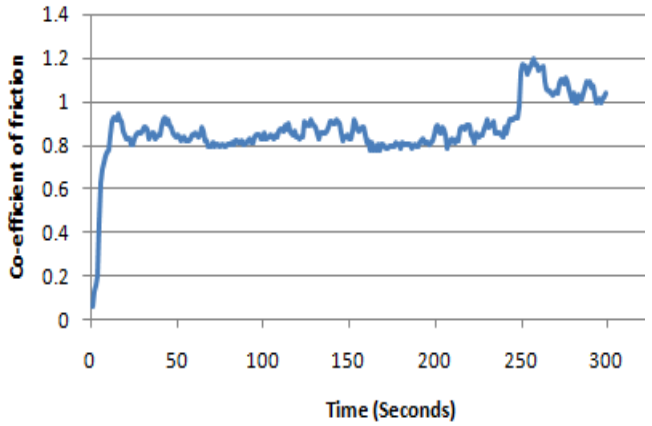

Fig. 2 (b) Dependency of co-efficient of friction with time. Material; high carbon high chromium steel. Load; 100N.

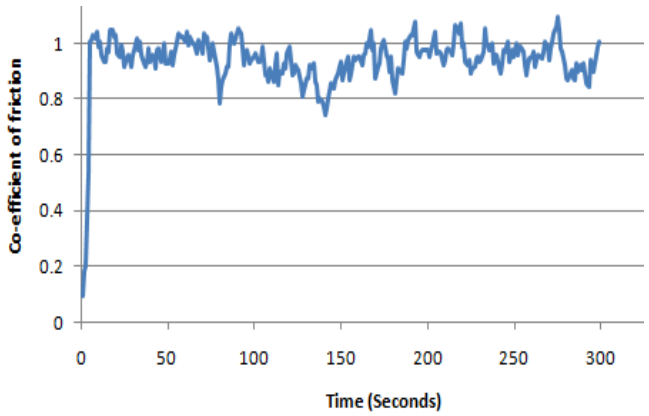

Fig. 2 (c) Dependency of co-efficient of friction with time. Material; Stainless steel. Load; 100N.

It is observed from Fig. 2 that co-efficient of friction for case hardened carbon steel and high carbon high chromium steel balls found to be steady after 30 seconds for a load of 100N. The steady state for stainless steel balls was reached approximately after 20 sec. The time required to reach steady state is called running in time.

The co-efficient of friction in Fig. 2 (a) and (b) stabilizes with respect to time except 2(c). This deviation in co-efficient of friction with time is depends on type of ball material. The average co-efficient of friction and the corresponding loads are shown in Table 4.

Table 4. Applied load and co-efficient of friction for different ball material.

Applied load (N)	Average Co-efficient of friction		
	Case hardened carbon steel	High carbon high chromium steel	Stainless steel
50	-	-	1.10
75	-	-	0.88
100	0.80	0.88	0.91
300	0.51	0.48	-
500	0.39	0.45	-

Average co-efficient of friction in case of case hardened carbon steel ball is 0.80, 0.51 and 0.39 for loads 100N, 300N and 500N. Average co-efficient of friction in case of high carbon high chromium steel ball is 0.88, 0.48 and 0.45 for loads 100N, 300N and 500N**.** The average co-efficient of friction in case of stainless steel ball is 1.10 and 0.88 for loads 50N and 75N. The average co-efficient of friction in case of stainless steel ball has been found to increase to 0.91 when load was changed to 100 N.

A plot depicting the variation of co-efficient of friction with normal load for stainless steel, high carbon high chromium steel and case hardened carbon steel balls are shown in Fig. 3.

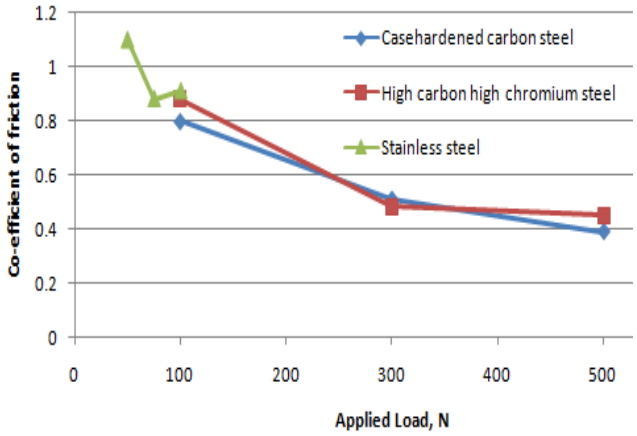

Fig. 3 Co-efficient of friction with applied load for different ball materials.

The co-efficient of friction for all ball materials under un-lubricated condition was found to decrease with increase in normal load. In case of stainless steel the co-efficient of friction decreased when normal load changed from 50N to 75N. The friction found to be saturated after 75 N.

Scanning electron microscope studies on wear track was carried out to understand the variation in co-efficient of friction with normal load.

B. Scanning electron micrographic studies on wear scar

The scanning electron micrographs of wear scar for stainless steel ball studied in scanning electron microscope for a normal load of 50N, 75N and 100N are shown in Fig. 4(a) to (f).

Published By:
Blue Eyes Intelligence Engineering and Sciences Publication (BEIESP)

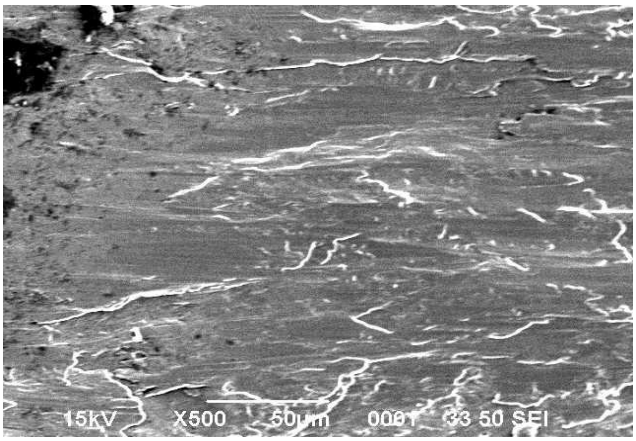

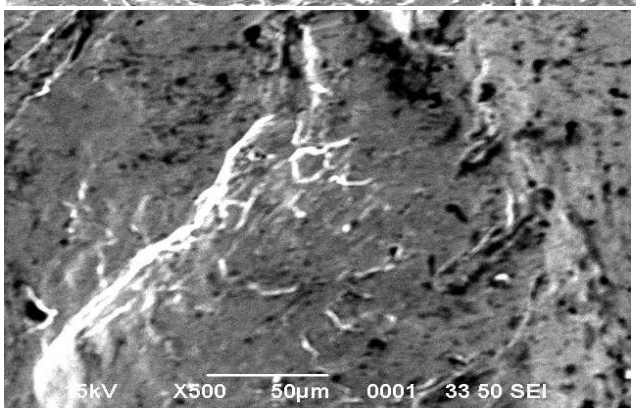

(a) Wear scar on lower ball Load; 50N Magnification; 500X (b) Wear scar on lower ball Load; 50N Magnification; 500X

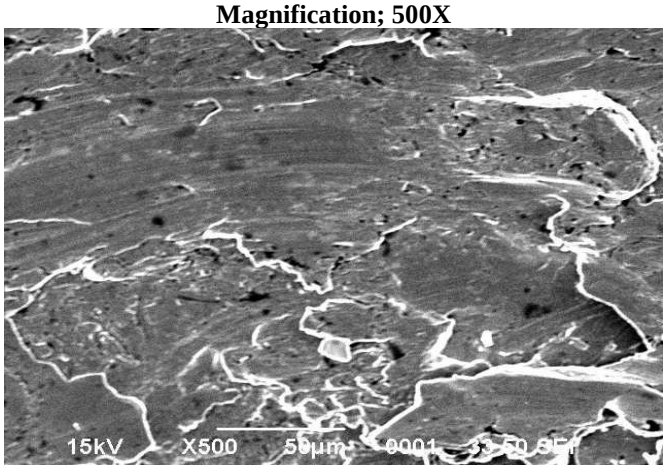

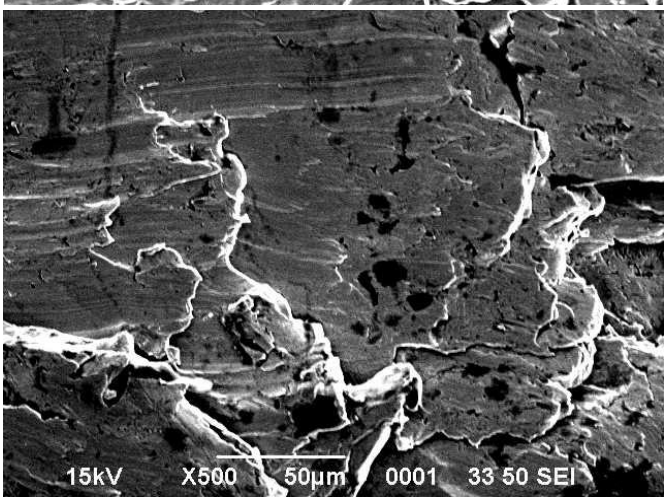

(c) Wear scar on lower ball Load; 75N Magnification; 500X (d) Wear scar on lower ball Load; 75N Magnification; 500X

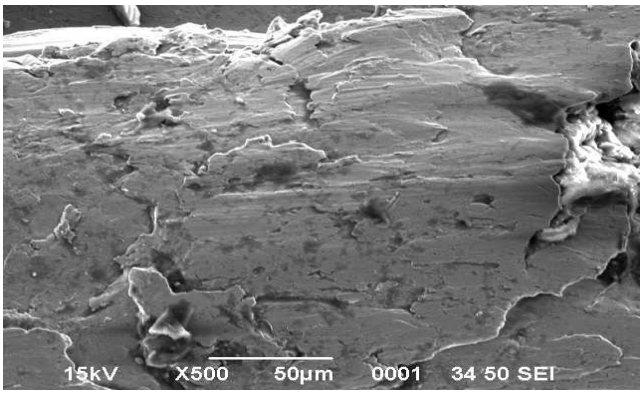

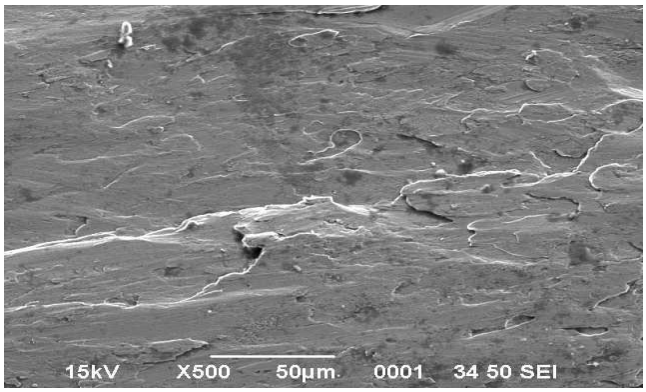

(e) Wear scar on lower ball Load; 100N Magnification; 500X (f) Wear scar on lower ball Load; 100N Magnification; 500X

Fig. 4 (a) to (f) Scanning electron micrographs of wear scar–stainless steel ball.

Micrograph shown in Fig. 4 (a) and (b) stands for 50N load are different compared to micrographs (c), (d), (e) and (f). Micrographs 4 (a) and (b) are more rough when compared to micrographs (c), (d), (e) and (f). The morphological feature of micrographs brings out the observed difference in variation of co-efficient of friction with normal load.

Micrograph 4 (a) shows that the damage occurring throughout the wear scar whereas micrograph 4(b) shows partial damage of the wear scar. Micrograph 4 (c) is more smooth when compared to micrograph 4 (d). In general the morphology of damage surfaces are comparable. Micrograph 4 (e) and (f) are comparable. The morphology of micrograph 4 (e) and (f) are comparable.

The scanning electron micrographs of wear scar for case hardened carbon steel ball studied in scanning electron microscope for a normal load of 100N, 300N and 500N are shown in Fig. 5(a) to (f)

Published By:
Blue Eyes Intelligence Engineering and Sciences Publication (BEIESP)

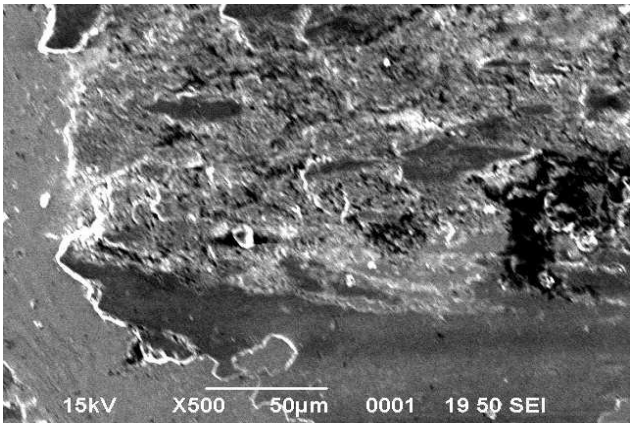

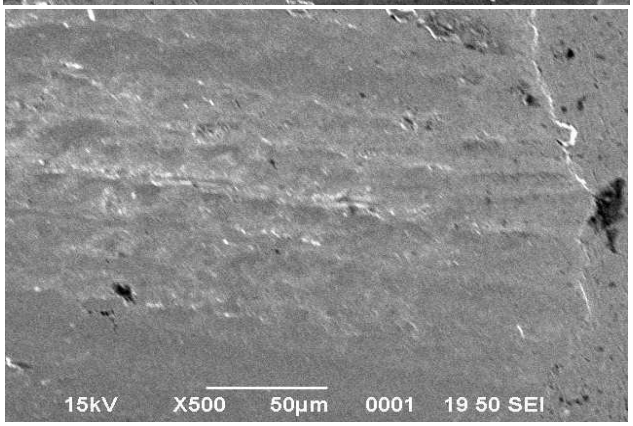

(a) Wear scar on lower ball Load; 100N Magnification; 500X (b) Wear scar on lower ball Load; 100N Magnification; 500X

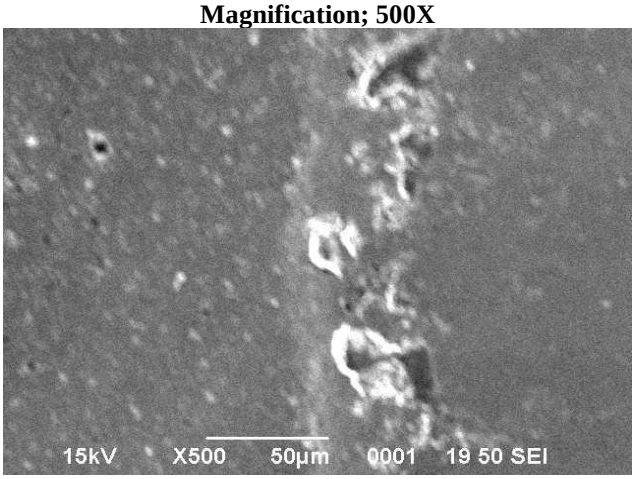

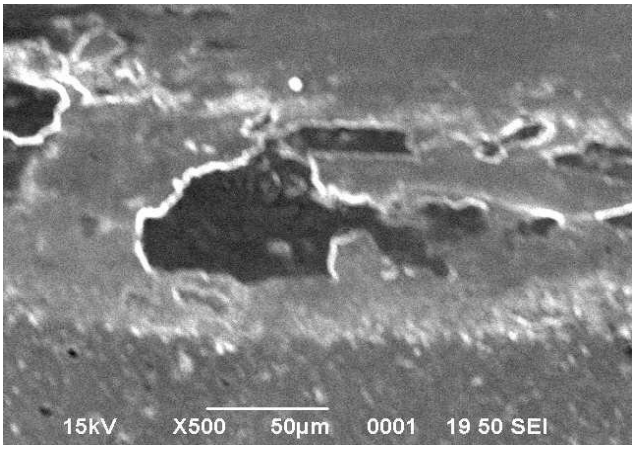

(c) Wear scar on lower ball Load; 300N Magnification; 500X (d) Wear scar on lower ball Load; 300N Magnification; 500X

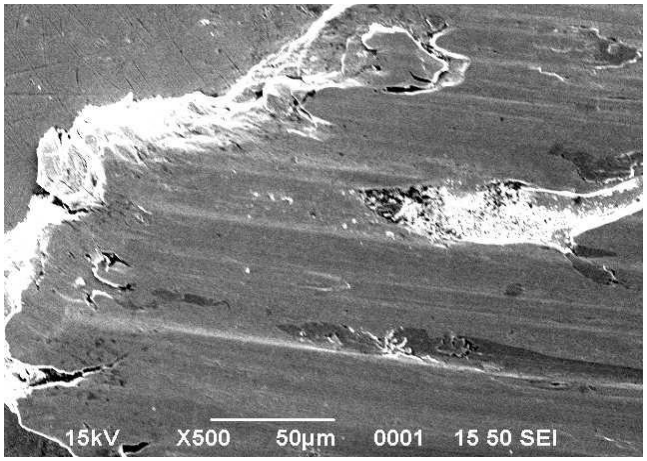

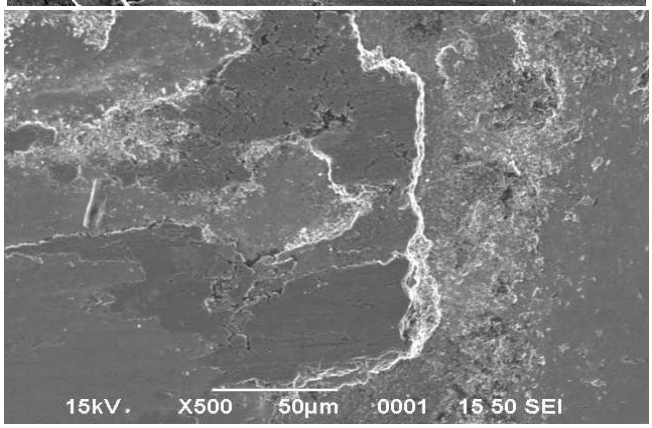

(e) Wear scar on lower ball Load; 500N Magnification; 500X (f) Wear scar on lower ball Load; 500N Magnification; 500X

Fig. 5 (a) to (f) Scanning electron micrographs of wear scar–case hardened carbon steel ball.

Micrograph 5 (a) and (b) stands for wear scar at 100N load. The morphological features of micrograph 5 (a) and (b) are not comparable. Micrograph 5 (b) is smoother compared to micrograph 5 (a). The deformations are uniform in wear scar of micrograph 5 (b) when compared to micrograph 5 (a).

Micrograph 5 (c) and (d) stands for wear scar at 300N load. The deformation in wear scar is distributed in wear scar area. The deformations are less when compared to micrographs 5 (a) and (b). The micrographs of 5 (c) and (d) are comparable. Micrograph 5 (e) and (f) corresponds to the wear scar of load 500N. The morphology and deformations are comparable in micrograph 5 (e) and (f).

The scanning electron micrographs of wear scar for high carbon high chromium steel ball studied in scanning electron microscope for a normal load of 100N, 300N and 500N are shown in Fig. 6(a) to (f)

Published By:
Blue Eyes Intelligence Engineering
and Sciences Publication (BEIESP)

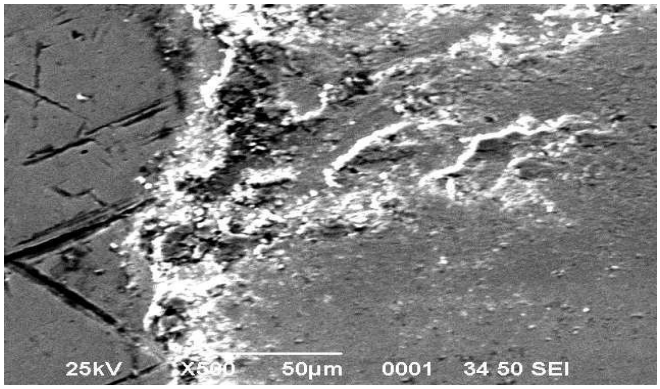

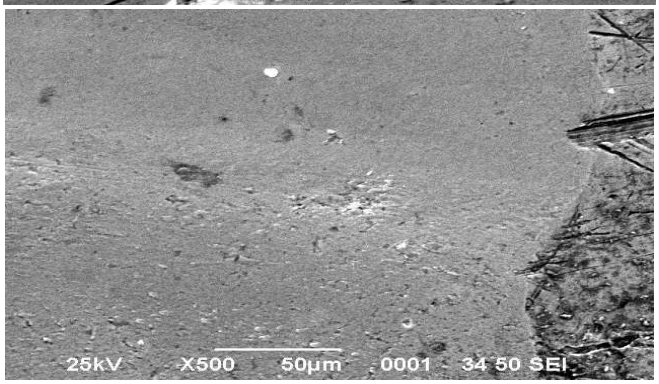

(a) Wear scar on lower ball Load; 100N Magnification; 500X (b) Wear scar on lower ball Load; 100N Magnification; 500X

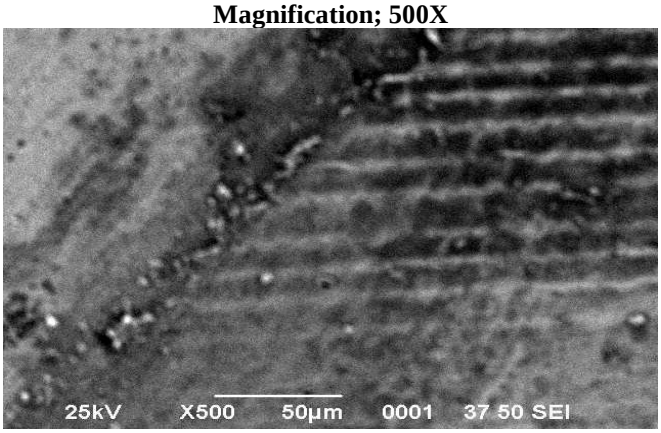

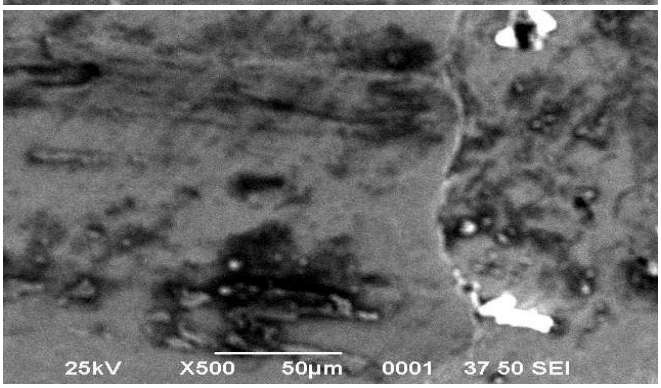

(c) Wear scar on lower ball Load; 300N Magnification; 500X (d) Wear scar on lower ball Load; 300N Magnification; 500X

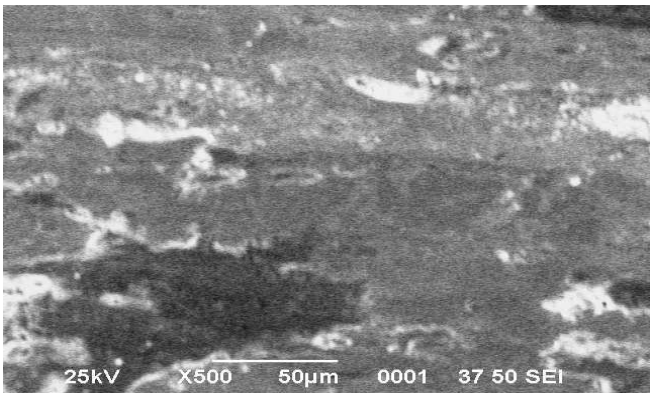

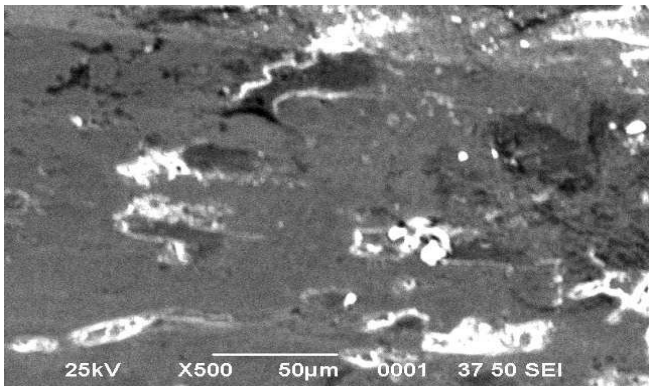

(e) Wear scar on lower ball Load; 500N Magnification; 500X (f) Wear scar on lower ball Load; 500N Magnification; 500X

Fig. 6 (a) to (f) Scanning electron micrographs of wear scar–high carbon high chromium steel ball.

Micrograph 6 (a) and (b) shows the wear scar at 100N load. The wear scars in micrograph 6 (a) corresponding to the beginning of wear path. Micrograph 6 (b) corresponds to the end of wear path except few patches at top left side of the wear scar in micrograph 6 (a), the other features of micrographs 6 (a) and (b) are comparable

Micrograph 6 (c) and (d) shows the wear scar at 300N load. Micrograph 6 (c) corresponds to the beginning portion of wear path. Micrograph 6 (d) corresponds to end of wear path. Micrograph 6 (c) shows non uniform deformations. Micrograph 6 (d) shows wear deformation appears to be uniform

Micrograph 6 (e) and (f) shows the wear scar at 500N load. Micrograph 6 (e) and micrograph 6 (f) are comparable and deformation is more uniform.

The micrographs for stainless steel ball element shown in Fig. 4 (a) to (f) are distinctively different when compared to micrographs shown in Fig. 5 (a) to (f) and Fig. 6 (a) to (f) which stands respectively for casehardened carbon steel and high carbon high chromium steel.

C. Tin coating on different substrates without lubricant

Dependency of co-efficient of friction with time for experiments where tin coating on case hardened carbon steel and high carbon high chromium steel balls are shown in Fig. 7.

Published By:
Blue Eyes Intelligence Engineering and Sciences Publication (BEIESP)

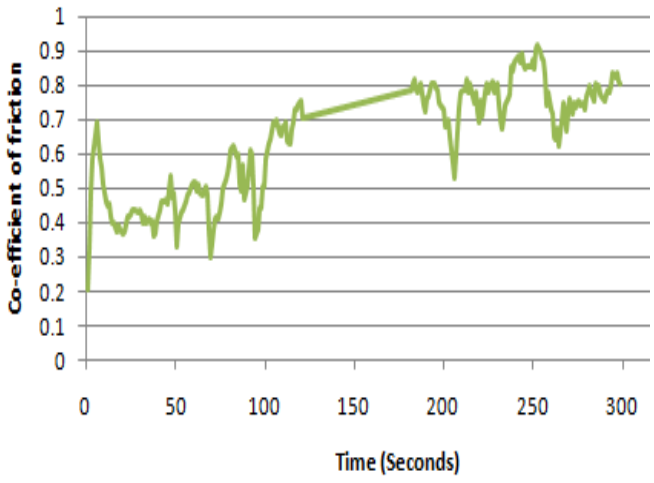

Fig. 7 (a) Dependency of co-efficient of friction with time. Material; Case hardened carbon steel (Tin coated) Load; 100N.

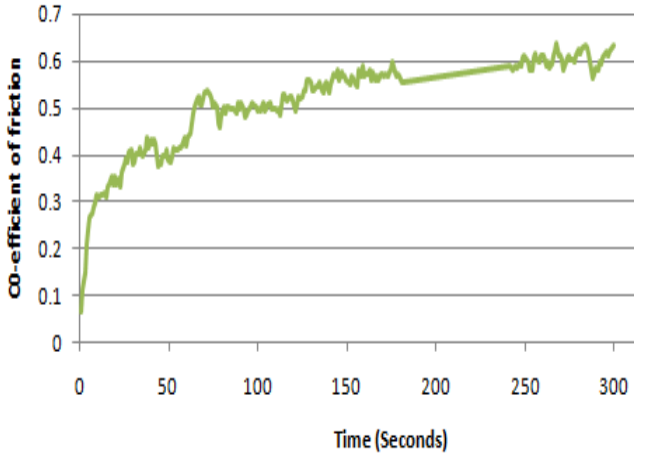

Fig. 7 (b) Dependency of co-efficient of friction with time. Material; high carbon high chromium steel (Tin coated) Load; 100N.

It is observed from Fig. 7 that co-efficient of friction for case hardened carbon steel balls (tin coated) was found to be steady after 100 seconds for a load of 100N. The steady state for tin coated high carbon high chromium steel balls was reached approximately after 100 seconds. The time required to reach steady state is called running in time.

The co-efficient of friction in Fig. 7 stabilizes with respect to time. This deviation in co-efficient of friction with time is attributed to total failure of coating and exposure of substrate. The average co-efficient of friction and the corresponding loads are shown in Table 5.

Table 5. Co-efficient of friction with applied load for tin coating on different ball materials.

Applied load (N)	Average co-efficient of friction	
	Case hardened carbon steel	High carbon high chromium steel
100	0.64	0.51
300	0.36	0.35
500	0.27	0.41

Average co-efficient of friction in case of case hardened carbon steel ball (tin coated) is 0.64, 0.36 and 0.27 for loads 100N, 300N and 500N. Average co-efficient of friction in case of high carbon high chromium steel ball (tin coated) is 0.51, 0.35 and 0.41 for loads 100N, 300N and 500N.

A plot depicting the variation of co-efficient of friction with normal load for casehardened carbon steel and high carbon high chromium steel balls are shown in Fig. 8.

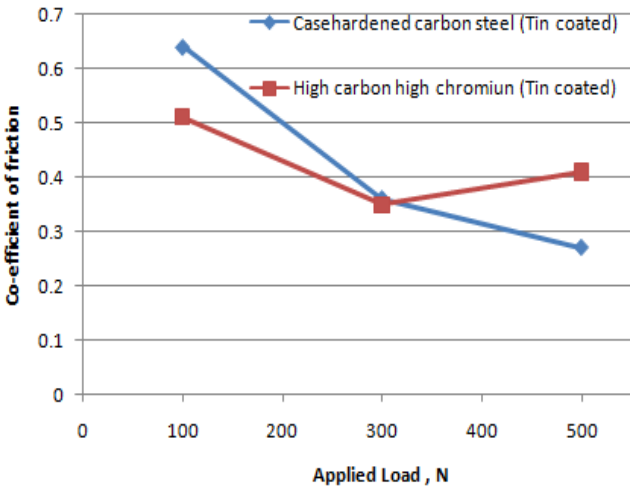

Fig. 8 Co-efficient of friction with applied load for case hardened carbon steel and high carbon high chromium steel balls (Tin coated)

In general the co-efficient of friction is comparable at any given load for both case hardened carbon steel and high carbon high chromium steel ball material. The co-efficient of friction was found to decrease with increase in normal load. The soft tin coating influence the deformation pattern which is reflected in values of co-efficient of friction at different normal load level.

For understanding the dependency of co-efficient of friction on the normal load, the wear scar was studied under scanning electron microscopy.

D. Scanning electron micrographic studies on wear scar

The scanning electron micrographs of wear scar for case hardened carbon steel ball (tin coated) studied in scanning electron microscope for a normal load of 100N, 300N and 500N are shown in Fig. 9(a) to (f)

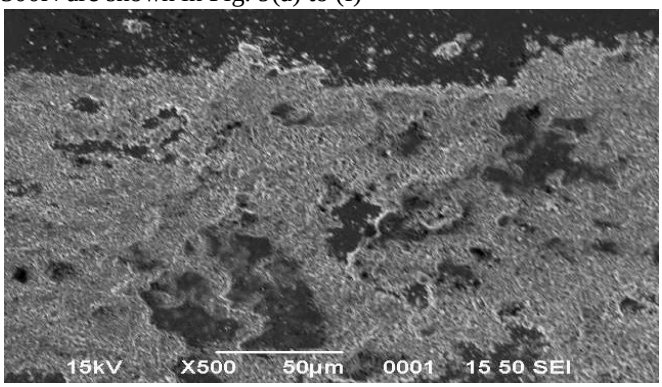

Published By:
Blue Eyes Intelligence Engineering
and Sciences Publication (BEIESP)

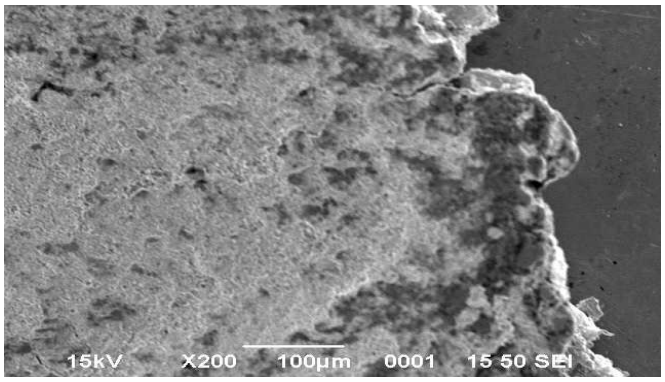

(a) Wear scar on lower ball Load; 100N Magnification; 500X

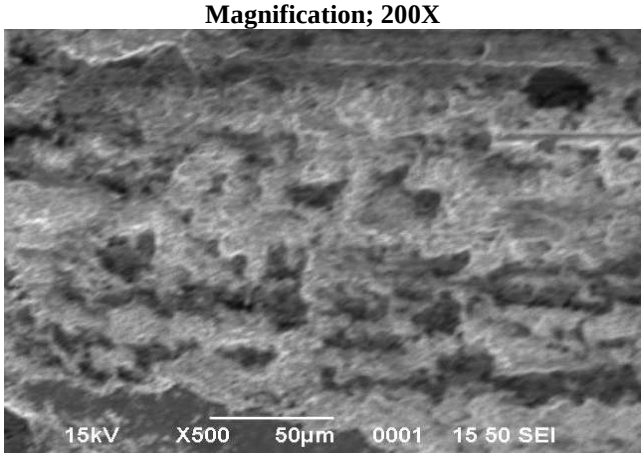

(b) Wear scar on lower ball Load; 100N Magnification; 200X

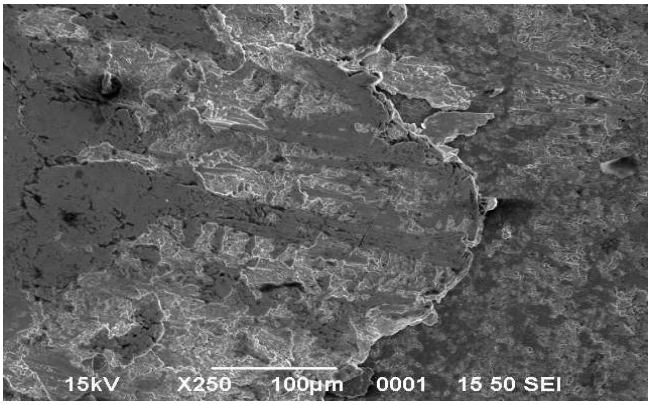

(c) Wear scar on lower ball Load; 300N Magnification; 500X

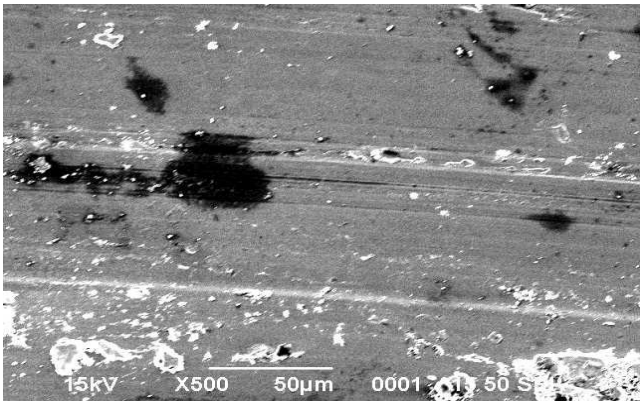

(d) Wear scar on lower ball Load; 300N Magnification; 250X

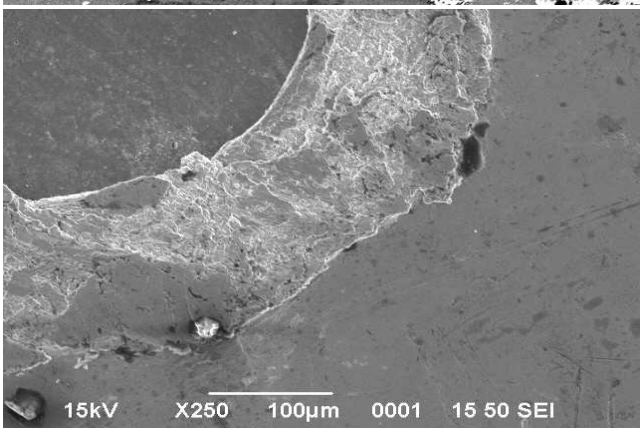

(e) Wear scar on lower ball Load; 500N Magnification; 500X

(f) Wear scar on lower ball Load; 500N Magnification; 250X

Fig. 9 (a) to (f) Scanning electron micrographs of wear scar-case hardened carbon steel. (Tin coated)

The micrographs 9 (a) and (b) corresponds to wear scar at 100N load. The morphological features of micrograph 9 (a) and (b) are comparable suggesting the deformations are also comparable. The micrograph 9 (c) and (d) corresponds to wear scar at 300N load. Micrograph 9(c) is studied at mid of the wear scar. Micrograph 9 (d) corresponds to end of the wear scar. The morphology and features of micrographs are not much similar.

The micrograph 9 (e) and (f) corresponds to wear scar at 500N load. Micrograph 9 (e) shows the deformation and morphology which are uniform. Micrograph 9 (f) shows the total failure of the coating and exposure of substrate.

The scanning electron micrographs of wear scar for high carbon high chromium steel ball (tin coated) studied in scanning electron microscope for a normal load of 100N, 300N and 500N are shown in Fig. 10 (a) to (f)

Published By:
Blue Eyes Intelligence Engineering and Sciences Publication (BEIESP)

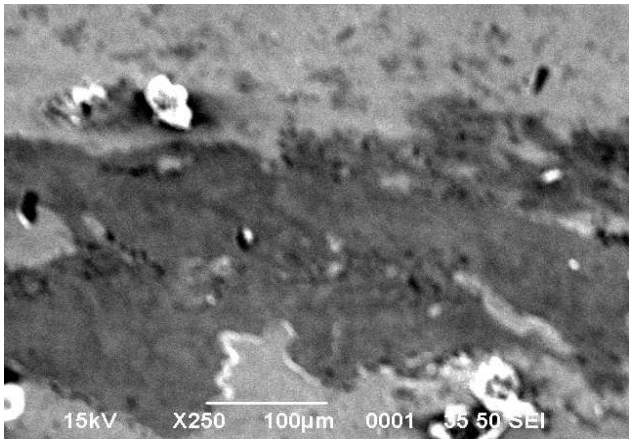

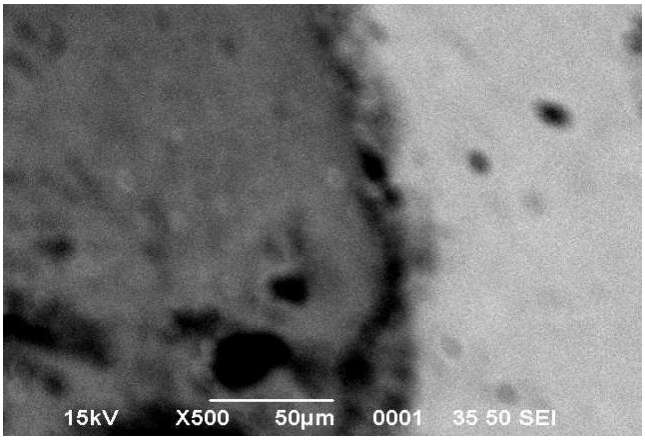

(a) Wear scar on lower ball Load; 100N Magnification; 250X (b) Wear scar on lower ball Load; 100N Magnification; 500X

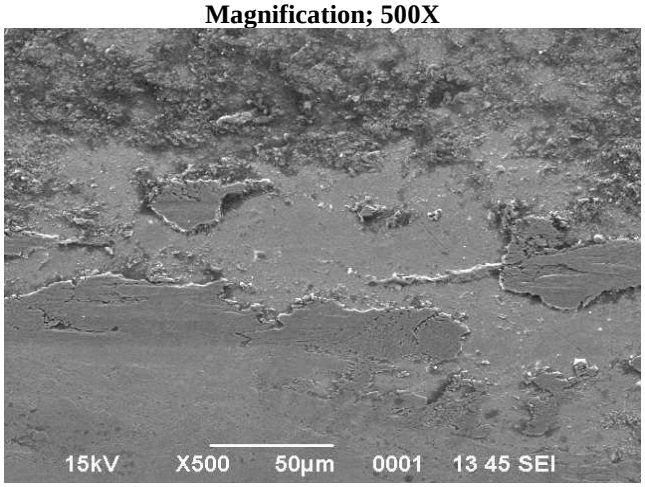

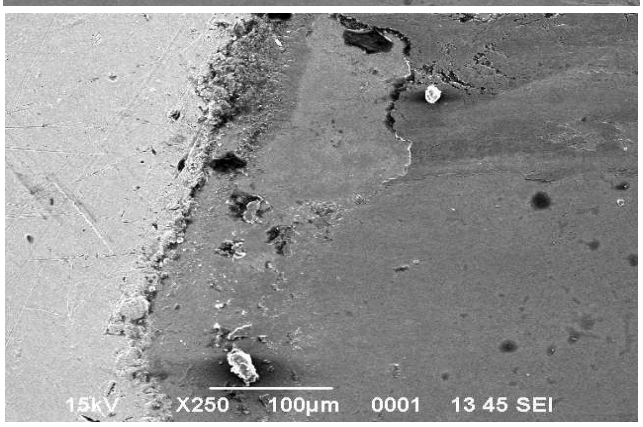

(c) Wear scar on lower ball Load; 300N Magnification; 500X (d) Wear scar on lower ball Load; 300N Magnification; 250X

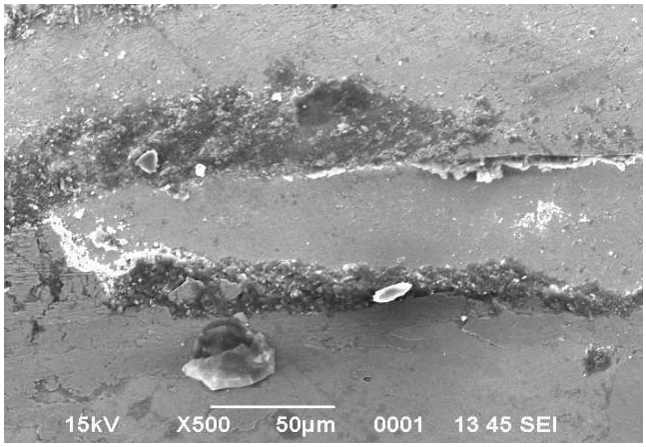

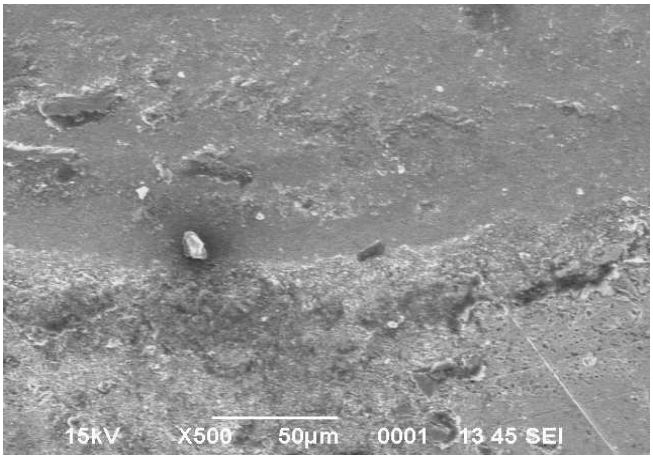

(e) Wear scar on lower ball Load; 500N Magnification; 500X (f) Wear scar on lower ball Load; 500N Magnification; 500X

Fig. 10 (a) to (f) Scanning electron micrographs of wear scar–high carbon high chromium steel ball. (Tin coated)

Micrograph 10 (a) and (b) shows the wear scar at 100N load. Micrograph 10 (a) corresponds to middle portion of the wear scar. Micrograph 10 (b) corresponds to end of the wear scar. The morphology and features in micrographs 10 (a) and (b) are comparable.

Micrograph 10 (c) and (d) shows the wear scar at 300N load. Micrograph 10 (c) corresponds to middle of the wear scar. Micrograph 10 (d) corresponds to end of the wear scar. The deformation and morphology are comparable to each other. The features in micrograph 10 (c) and (d) are uniform when compared to micrographs 10 (a) and (b).

Micrograph 10 (e) and (f) shows the wear scar at 500N load. Micrographs 10 (e) and (f) correspond to middle portion of the wear scar. The deformation and morphology are comparable to each other. The deformation and morphology are found to be more uniform in micrographs 10 (e) and (f) compared to micrographs 10(a), (b), (c) and (d).

These features in micrographs are attributed to the observed variation in co-efficient of friction with normal load.

E. Zinc coating on different ball materials without lubricant

Dependency of co-efficient of friction with time for experiments where zinc coating on case hardened carbon steel and stainless steel balls were shown in Fig. 11.

Published By:
Blue Eyes Intelligence Engineering
and Sciences Publication (BEIESP)

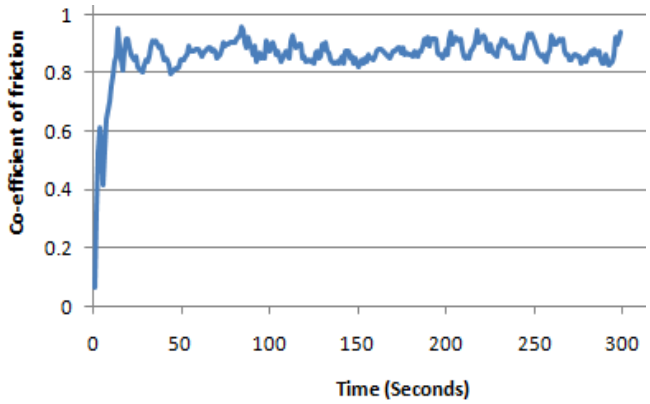

Fig. 11 (a) Dependency of co-efficient of friction with time. Material; Case hardened carbon steel (Zinc coated) Load; 100N.

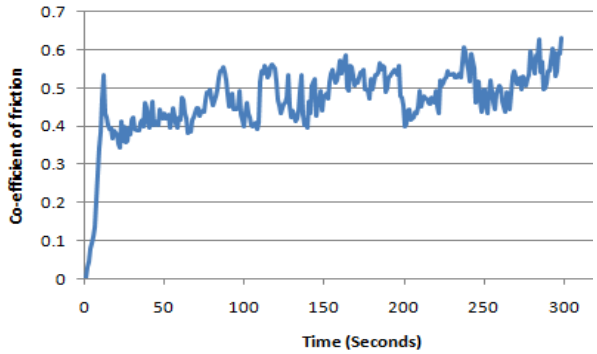

Fig. 11 (b) Dependency of co-efficient of friction with time. Material; Stainless steel (Zinc coated) Load; 100N.

It is observed from Fig. 11 that co-efficient of friction for case hardened carbon steel balls (zinc coated) was found to be steady after 20 seconds for a load of 100N. The steady state for zinc coated stainless steel balls was reached approximately after 30 seconds for a load of 100N. The time required to reach steady state is called running in time.

The co-efficient of friction in Fig. 11 stabilizes with respect to time. This deviation in co-efficient of friction with time is attributed to total failure of coating and exposure of substrate. The average co-efficient of friction and the corresponding loads are shown in Table 6.

Table 6. Co-efficient of friction with applied load for zinc coating on different ball materials.

Applied load (N)	Average co-efficient of friction	
	Case hardened carbon steel	Stainless steel
50	-	0.73
75	-	0.60
100	0.87	0.51
300	0.54	-
500	0.36	-

Average co-efficient of friction in case of case hardened carbon steel ball (zinc coated) is 0.87, 0.54 and 0.36 for loads 100N, 300N and 500N. Average co-efficient of friction in case of stainless steel ball (zinc coated) is 0.73, 0.60 and 0.51 for loads 50N, 75N and 100N.

A plot depicting the variation of co-efficient of friction with normal load for case hardened carbon steel and stainless steel balls are shown in Fig. 12.

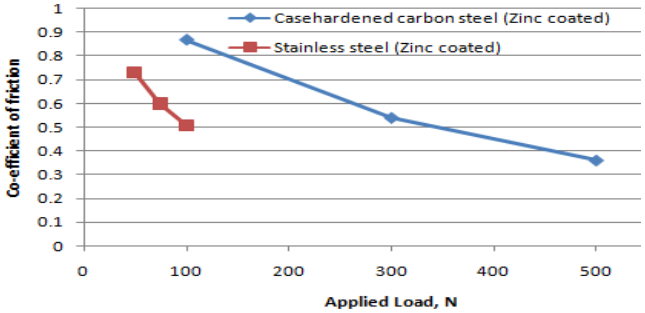

Fig. 12 Co-efficient of friction with applied load for case hardened carbon steel and stainless steel balls (Zinc coated)

The co-efficient of friction for both case hardened carbon steel and stainless steel were found to decrease with increase in normal load. The rate of decrease is more for stainless steel balls which are softer. The rate of decrease in co-efficient of friction with normal load for case hardened carbon steel is less compare to stainless steel. At a given load the co-efficient of friction for case hardened carbon steel is more compared to stainless steel elements. This is attributed to difference in hardness of casehardened carbon steel and stainless steel balls.

For understanding the dependency of co-efficient of friction with load, scanning electron microscope study was carried out on wear scar.

F. Scanning electron micrographic studies on wear scar

The scanning electron micrographs of wear scar for stainless steel ball (zinc coated) studied in scanning electron microscope for a normal load of 50N, 75N and 100N are shown in Fig.13 (a) to (f)

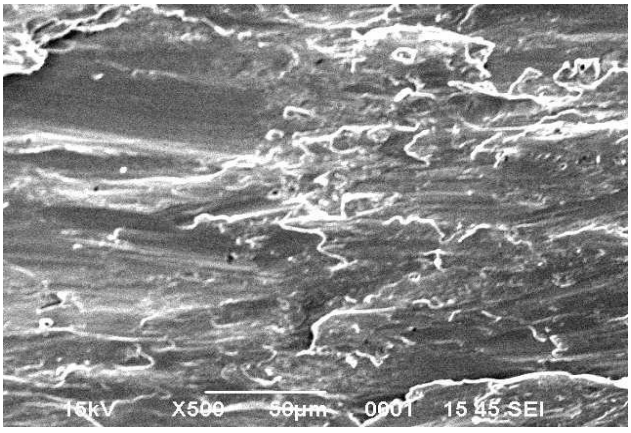

Published By:
Blue Eyes Intelligence Engineering
and Sciences Publication (BEIESP)

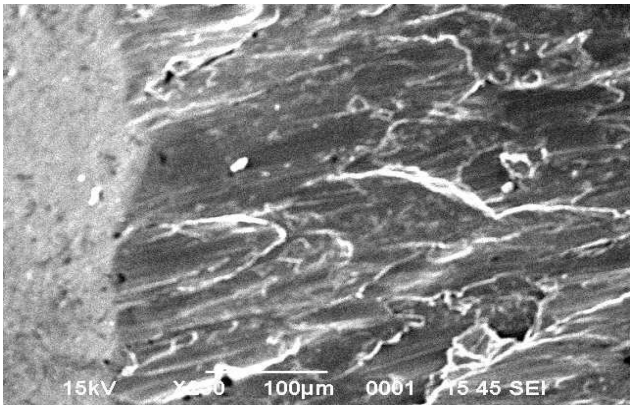

(a) Wear scar on lower ball Load; 50N Magnification; 500X

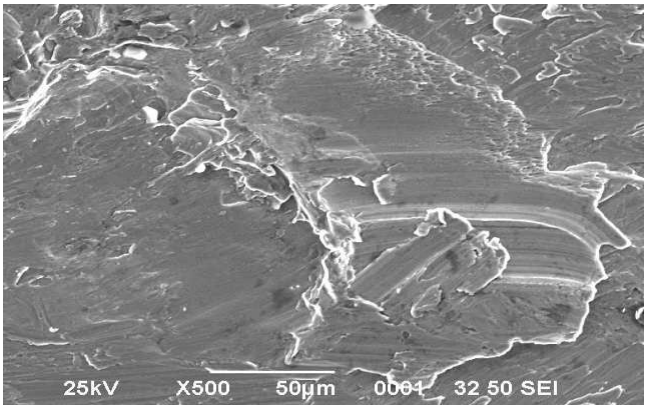

(b) Wear scar on lower ball Load; 50N Magnification; 500X

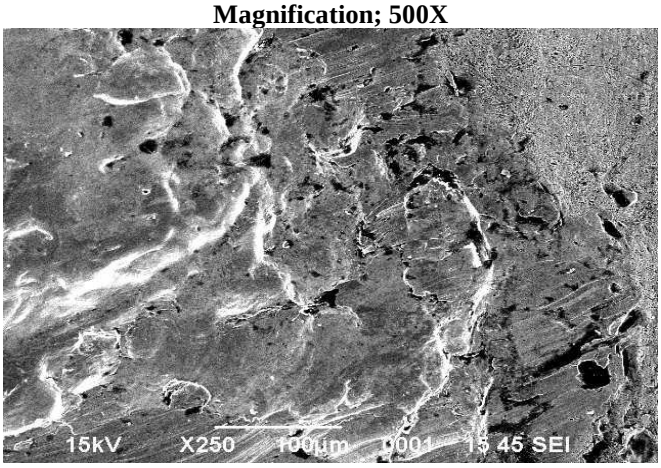

(c) Wear scar on lower ball Load; 75N Magnification; 250X

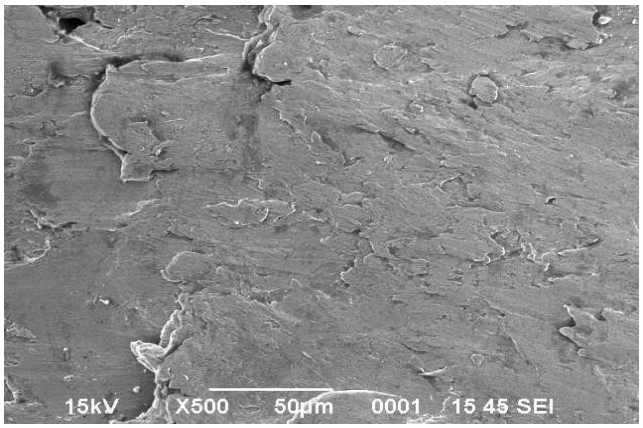

(d) Wear scar on lower ball Load; 75N Magnification; 500X

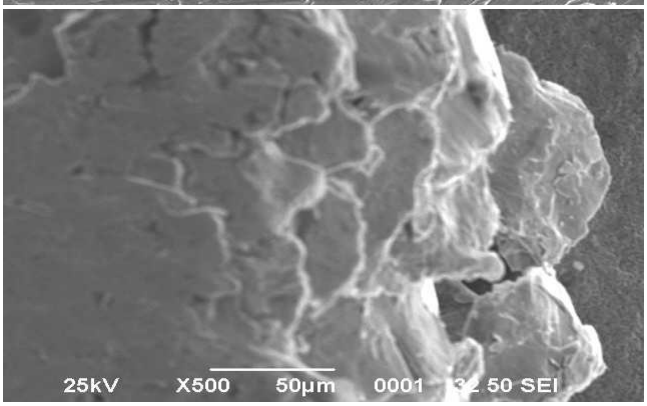

(e) Wear scar on lower ball Load; 100N Magnification; 500X

(f) Wear scar on lower ball Load; 100N Magnification; 500X

Fig. 13 (a) to (f) Scanning electron micrographs of wear scar–stainless steel ball. (Zinc coated)

Micrograph 13 (a) and (b) shows the wear scar at 50N load. Micrograph 13 (a) corresponds to middle of the wear scar. Micrograph 13 (b) corresponds beginning of wear scar. The morphology and features of micrographs 13 (a) and (b) are comparable to each other.

Micrograph 13 (c) and (d) shows the wear scar at 75N load. Micrograph 13 (c) corresponds to end of the wear scar. Micrograph 13 (d) corresponds to middle of the wear scar. The features in micrograph 13 (c) and (d) are more uniform and smooth compared to micrographs 13 (a) and (b).

Micrograph 13 (e) and (f) shows the wear scar at 100N load. The features in micrograph 13 (e) and (f) are more comparable to each other. These features are also similar to micrographs 13 (c) and (d).

The scanning electron micrographs of wear scar for case hardened carbon steel ball (zinc coated) studied in scanning electron microscope for a normal load of 100N, 300N and 500N are shown in Fig. 14 (a) to (f)

Published By:
Blue Eyes Intelligence Engineering
and Sciences Publication (BEIESP)

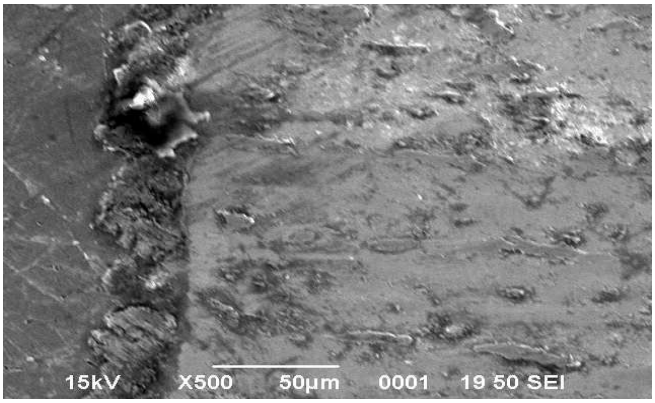

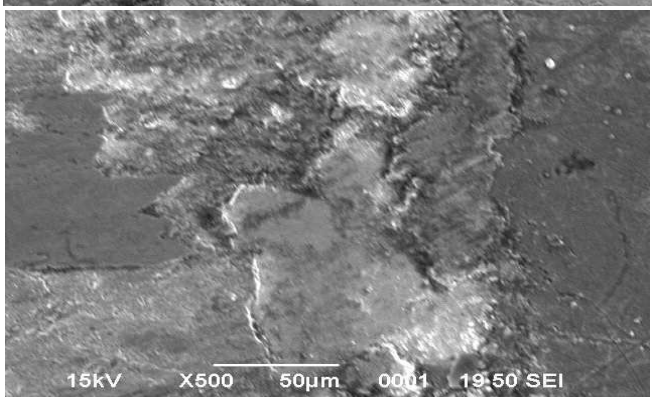

(a) Wear scar on lower ball Load; 100N Magnification; 500X (b) Wear scar on lower ball Load; 100N Magnification; 500X

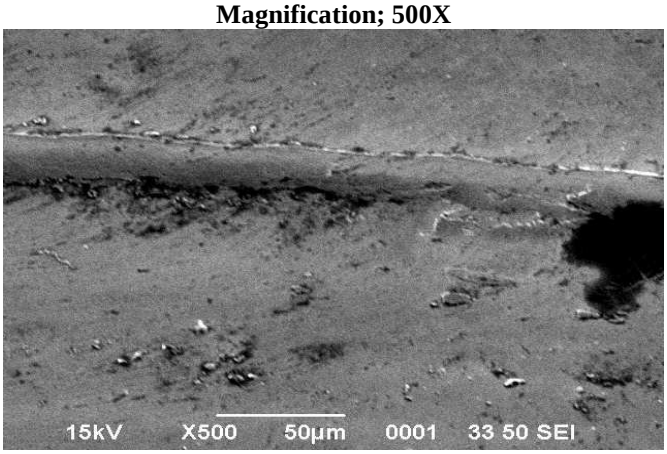

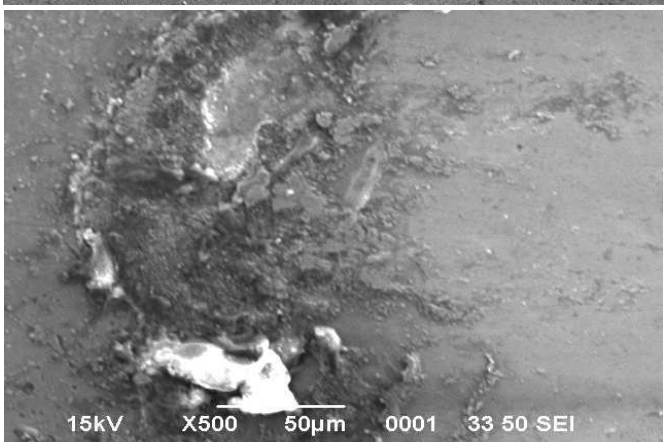

(c) Wear scar on lower ball Load; 300N Magnification; 500X (d) Wear scar on lower ball Load; 300N Magnification; 500X

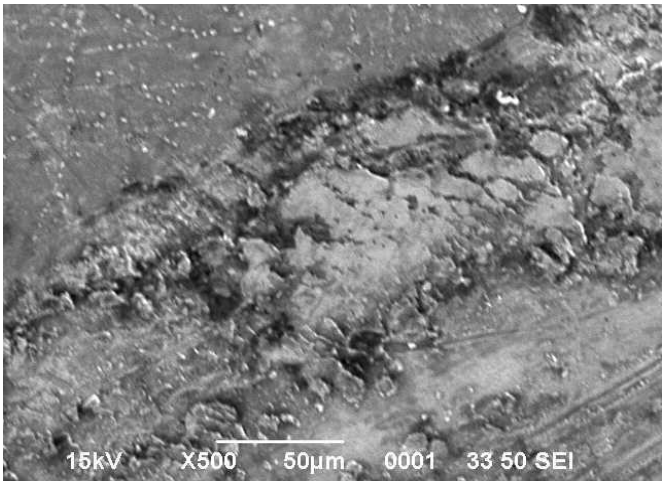

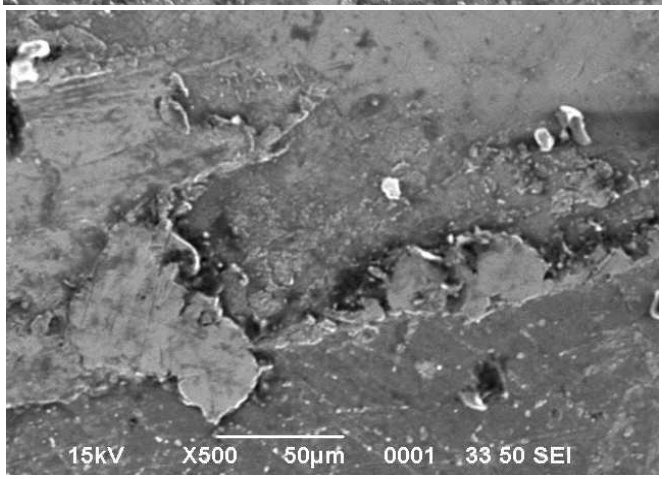

(e) Wear scar on lower ball Load; 500N Magnification; 250X (f) Wear scar on lower ball Load; 500N Magnification; 500X

Fig. 14 (a) to (f) Scanning electron micrographs of wear scar–case hardened carbon steel. (Zinc coated)

Micrograph 14 (a) and (b) shows the wear scar at 100N load. Micrographs 14 (a) and (b) are comparable to each other and deformations are not uniform. Micrograph 14(c) and (d) shows the wear scar at 300N load. The features in micrographs 14 (c) and (d) are not very comparable. The feature in micrograph 14 (c) is smoother and not widely observed. The features in micrograph 14 (d) are more intense compared features in micrograph 14 (c).

Micrograph 14 (e) and (f) shows the wear scar at 300N load. The features in micrographs 14 (e) and (f) are comparable. These features in micrograph 14(e) and (f) are comparable to features observed in micrograph 14 (d).

The different morphology and features observed in scanning electron micrographs collaborate the variation in co-efficient of friction with respect to normal load, type of coating and substrate materials.

IV. CONCLUSIONS

1. In case of un-lubricated condition the co-efficient of friction decreases with increase in applied normal load. The rate of decrease is at higher load level compared to lower load levels.

Published By:
Blue Eyes Intelligence Engineering
and Sciences Publication (BEIESP)

2. The hardness of the material was found to influence the friction coefficient and deformation features.
3. The hardness of the substrate was found to play a role in soft coated un-lubricated conditions.
4. The normal load was also to have a role in performance of elements coated with soft material like tin.
5. The hardness of the substrate material was found to influence the performance of the ball element.
6. The normal load was also found to influence the deformation and performance of ball element.

REFERENCES

1. R. Ahmed and M. Hadfield, Wear 203/204 (1997) 98–106.
2. Makela, P. Vouristo, M. Lahdensuo, K. Niemi and T. Mantyla, Proceedings of the 7th International Thermal Spray Conference, Boston,
3. Massachuesetts, 20–24 June 1994, pp. 759–763.
4. M. Faraday, Philos. Trans. R. Soc. 147 (1857) 145.
5. K. Kirner, Schweissen Schnieden 41 (1989) 583–586.
6. M.E. Vinayo, F. Kassabji, J. Guyonnet and P. Fauchais, J. Vac. Sci. Technol. A3 (1985) 2483–2489.
7. J. Nerz, B.A. Kushner and A.J. Rotolico, Proceedings of the Thermal Spraying Conference, Essen, Germany, 29–31 August 1990, pp. 47–
8. 51.
9. M.P. Subrahmanyam, M.P. Srivastava and R. Sivakumar, Mater. Sci. Eng. 84 (1984)209–214.
10. R. Nieminen, P. Vouristo, K. Niemi, T. Mantyla and G. Barbezat, Wear 212 (1997) 66–77.
11. R. Ahmed and M. Hadfield, Tribol. Int. 30 (1997) 129–137.
12. R. Ahmed and M. Hadfield, Surf. coatings Technol. 82 (1996) 176–186.
13. R. Ahmed and M. Hadfield, Wear 230 (1999) 39–55.
14. S. Tobe, S. Kodama and H. Misawa, Proceedings of the National Thermal Spray Conference, Tokoyo, Japan, 1990, pp. 171–178.
15. R. Ahmed and M. Hadfield, Proceedings of the International Thermal Spray Conference, Singapore, ISBN 0871707373, 2001, pp. 1009–
16. 1015.
17. M. Yoshida, K. Tani, A. Nakahira, A. Nakajima and T. Mawatari, Proceedings of ITSC, Kobe, May 1995, 1992, pp. 663–668.
18. R. Ahmed and M. Hadfield, Wear 209 (1997) 84–95.
19. Nakajima, T. Mawatari, M. Yoshida, K. Tani and A. Nakahira, Wear 241 (2000) 166–173.
20. S. Kuroda, T. Fukishima and S. Kitahara, Proceedings of the International Thermal Spray Conference, Orlando,OH, 1992, pp. 903–909.
21. T. Morishita, E. Kuramochi, R.W. Whitfield and S. Tanabe, Proceedings of the International Thermal Spray Conference, Orlando, OH, 1992, pp. 1001–1004.
22. O.C. Brandt, J. Therm. Spraying 4 (1995) 147–152.
23. G.R. Millar, L.M. Keer and H.S. Cheng, Proc. R. Soc. London, Ser. A 397 (1985) 197–209.
24. T.A. Harris, Rolling Bearing Analysis, 3rd ed., Wiley, New York, 1991, p. 23.
25. H.S. Cheng, T.P. Chang and W.D. Sproul, Proceedings of the 16th Leeds–Lyon Symposium, Elsevier, 1990, pp. 81–88.
26. R. Thom, L. Moore, W.D. Sproul and T.P. Chang, Surf. Coatings Technol. 62 (1993) 423–427.
27. O. Knolek, B. Bosserhoff, A. Schrey, T. Leyendecker, O. Lemmer and S. Esser, Surf. Coating Technol. 54/55 (1992) 102–107.
28. L. Rosado, V.K. Jain and H.K. Trivedi, Wear 212(1997) 1–6.
29. I.A. Polonsky, T.P. Chang, L.M. Keer and W.D. Sproul, Wear 208 (1997) 204–219.
30. Suresha Gowda M. V, Vidyasagar H. N and Ranganatha S, IJRTE, ISSN: 2277-3878,Vol 4 Jan 2016, 1-8.
31. Suresha Gowda M. V, Ranganatha S and Vidyasagar H. N, IJITEE, ISSN: 2278-3075, Vol 5, Feb 2016, 24-31.

Suresha Gowda M. V., Graduated in BE (Mechanical Engineering), completed ME (Machine Design) and pursuing research in the Department of Mechanical Engineering, University Visweswaraya College of Engineering, Bangalore. Working as an Assistant Professor in the Department of Mechanical Engineering, S. J. C. Institute of Technology, Chick ballapur, Karnataka.

Dr. Ranganatha S., Graduated in BSc (MU), BE (Metallurgy), ME (Mechanical) and PhD from IISc. Bangalore. Working as Professor in the Department of Mechanical Engineering, University Visweswaraya College of Engineering, Bangalore, Karnataka.

Dr. Vidyasagar H. N., Graduated in BE (Mechanical Engineering), completed M.Tech (Advanced Manufacturing Engineering) and PhD from UVCE Bangalore. Working as an Associate Professor in the Department of Mechanical Engineering, University Visweswaraya College of Engineering, Bangalore, Karnataka.

Published By:
Blue Eyes Intelligence Engineering and Sciences Publication (BEIESP)